Title	10 Hz periodic component influences lower frequency component of the physiological tremor at low force levels
Author(s)	Endo, Hiroshi; Kawahara, Koichi
Citation	European Journal of Applied Physiology, 111(11), 2695-2705 https://doi.org/10.1007/s00421-011-1903-6
Issue Date	2011-11
Doc URL	http://hdl.handle.net/2115/50374
Rights	The original publication is available at www.springerlink.com
Type	article (author version)
File Information	EJAP111-11_2695-2705.pdf

Title

10-Hz periodic component influences lower frequency component of the physiological tremor at low force levels

Authors

Hiroshi Endo (Corresponding Author)

Multimodal Integration Research Group, Human Technology Research Institute,

National Institute of Advanced Industrial Science and Technology (AIST)

1-1-1 Higashi, Tsukuba, Ibaraki, 305-8566, Japan

Tel : +81-29-861-6661   Fax: +81-29-861-6662

e-mail: hiroshi-endou@aist.go.jp

Koichi Kawahara

Laboratory of Cellular Cybernetics, Graduate School of Information Science and

Technology, Hokkaido University

Kita 14, Nishi 9, Kita-ku, Sapporo, Hokkaido, 060-0814, Japan

Tel & Fax: +81-11-706-7591

e-mail: kawahara@ist.hokudai.ac.jp

Abstract

A positive correlation has been reported between the amplitudes of the 10-Hz and lower frequency components of the physiological tremor (PT) at low force levels, though the generation mechanisms based on motor unit (MU) firing properties are different. This study aimed to investigate the causal relation between these fluctuations. A computer simulation was performed to alter the fluctuation intensity, which enabled manipulation of MU firing properties. Two types of MU contributions to synchronization activity were considered to influence the intensity of the 10-Hz PT: (1) number of MUs involved in synchronization and (2) synchrony between MUs. The impact of oscillatory excitatory input from the central nervous system on the generation of the 10-Hz PT was also evaluated. The results showed that the lower frequency fluctuation (LF fluctuation) was influenced by the number of MUs contributing to the 10-Hz PT amplitude. The synchrony between MUs and the oscillatory excitatory input had no influence on the LF fluctuation. In conclusion, MU synchronization in a certain frequency range increased the fluctuations not only at the synchronizing frequency but also at lower frequencies, and the number of MUs involved in synchronization was a plausible factor to explain the correlation between the 10-Hz and LF fluctuations.

Keywords

1. Introduction

When an individual performs a position- or force-holding task, muscle forces fluctuate around an average value as a result of motor control uncertainty. These fluctuations, observed in normal individuals, are known as the physiological tremor (PT). Though fluctuation amplitude has been shown to correlate positively with muscle force (Moritz et al. 2005; Taylor et al. 2003), the amplitude in the frequency domain is more damped at higher frequencies (Christakos et al. 2006; Erimaki and Christakos 1999; Sowman and Türker 2005; Taylor et al. 2003). For example, the amplitude of finger force fluctuation was shown to fall off at approximately −30 dB/decade in the squared power spectrum around 10 Hz (approximately between 1 and 30 Hz) (Allum et al. 1978; Endo and Kawahara 2010). In other words, the force fluctuation is dominated by low frequency components up to 5 Hz.

It has also been shown that there are several frequency peaks in the PT (Christakos et al. 2006; Elble 1996; Halliday et al. 1999; McAuley and Marsden 2000; McAuley et al. 1997; Takanokura and Sakamoto 2001; Vaillancourt and Newell 2000). For example, finger tremors show oscillations at 10, 20, and 40 Hz (McAuley et al. 1997; Takanokura and Sakamoto 2001; Vaillancourt and Newell 2000). The 10-Hz component is the most common frequency peak in neurophysiologic tremors, which are associated with peaks ranging between 6 Hz and 12 Hz (Christakos et al. 2006; Elble 1996; McAuley and Marsden 2000). The 20-Hz component of finger tremors is due to oscillations caused by mechanical resonance observed in postural tremors. The 40-Hz component is also neurological but cannot always be detected clearly (McAuley et al. 1997). During a force-holding task, the frequency peak around 10 Hz is often observed in the power spectrum of fluctuations (Christakos et al. 2006; Elble and Randall 1976; McAuley and Marsden 2000; McAuley et al. 1997; Semmler and Nordstrom 1995, 1998). To sum up, the

fluctuation that is composed of low frequency components is the dominant component of force tremors, and the fluctuation that oscillates around 10 Hz appears as a second prominent component.

Interestingly, the amplitude of the 10-Hz fluctuation was reported to correlate with the intensity of fluctuations at low force levels (Endo and Kawahara 2010; Vasilakos et al. 1998). A positive correlation between fast Fourier transform (FFT) peak amplitudes of the 10-Hz fluctuation and standard deviations (SDs) of the lower frequency component of fluctuations was observed in force-holding tasks (Endo and Kawahara 2010), while a positive correlation between RMS values of the 10-Hz fluctuation and SDs of total fluctuation was observed in finger position−holding tasks (Vasilakos et al. 1998).

As for generation mechanisms, the 10-Hz fluctuation component of the PT is results from neurophysiologic sources, that is, synchronized motor unit (MU) oscillations (Christakos et al. 2006; Erimaki and Christakos 1999; Halliday et al. 1999) and/or common oscillatory excitatory input from the central nervous system to a motoneuron pool (McAuley et al. 1997; Raethjen et al. 2002; Wessberg and Vallbo 1996). On the other hand, though sources of the low frequency fluctuation of the PT are obscure, the performance of voluntary motor control with visual feedback (Mityake et al. 2001; Vasilakos et al. 1998) and involuntary muscle force fluctuations (Moritz et al. 2005; Taylor et al. 2003) are considered to be involved. As for a cause of muscle force fluctuations, discharge rate variability of MUs has been reported to contribute to force fluctuations (Laidlaw et al. 2000; Moritz et al. 2005; Taylor et al. 2003; Tracy et al. 2005). Discharge rate variability of the last-recruited largest-size MUs is a determinant of force fluctuations (Moritz et al. 2005). The above mechanism has been shown to account well for age-related differences in fluctuations, specifically the fact that older adults show larger fluctuations and greater variability in MU discharge rates compared with younger adults (Laidlaw et al. 2000; Tracy et al. 2005).

Because it is difficult to explain all the fluctuation components of the PT using a single MU

firing property, some uncertainty remains concerning the relation between the amplitudes of 10-Hz and

lower frequency fluctuations. Therefore, this study aimed to evaluate the causal relation between the

10-Hz and lower frequency fluctuations. In order to alter fluctuation amplitudes based on the above

mechanisms, it is necessary to change MU discharge properties. Due to the difficulty in directly

manipulating these properties, we utilized a computer simulation in this study. Because the correlation

between the 10-Hz and lower frequency fluctuations was observed at low force levels and it has been

reported that fluctuations and control strategies differ between low and moderate force levels (Moritz et al.

2005; Sosnoff et al. 2006; Taylor et al. 2003), the simulation was performed at a 10% MVC (maximal

voluntary contraction) force level. To demonstrate muscle force fluctuations, Fuglevand's motor unit

model was adopted (Fuglevand et al. 1993). The 10-Hz fluctuation of the PT was based on MU

synchronization and excitatory input from the CNS.

2. Methods

2.1. Motor unit model

A model of MU recruitment and rate coding, originally developed by Fuglevand et al. (1993),

was used to simulate the isometric force produced by a pool of MUs. The model parameters have been

modified to fit actual measurement data (Moritz et al. 2005; Taylor et al. 2003; Taylor et al. 2002; Yao et

al. 2000). Moritz et al. (2005) were able to demonstrate the coefficient of variation (CV) for force,

especially at low forces that previous reports failed to simulate, and for the most part their parameters were used in this study.

In brief, whole muscle force was calculated as the linear sum of single MU forces. Single MU forces were derived as the impulse response of an action potential (Fuglevand et al. 1993). The number of MUs included in the pool was 180 (Moritz et al. 2005) and a 100-fold range of twitch forces was used (Fuglevand et al. 1993), where MU 1 was the first recruited, had the smallest twitch force [1 arbitrary unit (au)], and the longest contraction time (90 ms). MU 180 was the last recruited, and had the largest twitch force (100 au) and shortest contraction time (30 ms). The twitch forces of other MUs were distributed exponentially, with contraction time depending on twitch force (an inverse power function) (Fuglevand et al. 1993).

MUs were recruited when the excitatory input from the CNS, E_{in}, went over the recruitment threshold of each MU. Recruitment thresholds were determined based on an exponential function with a 12-fold range, with arbitrary excitation units from MU 1 to MU 180 (Yao et al. 2000), where MU 180 was recruited at 59% MVC.

The minimum discharge rate was set at 7.6 pps (pulses per second) for MU 1 and increased linearly with recruitment threshold to 17.9 pps for MU 180 (Moritz et al. 2005). The maximal discharge rate also increased linearly from 17.6 to 34.8 pps (Moritz et al. 2005). Variability in discharge rate, that is, the CV for the interspike interval (ISI), which was the most important property in simulating the low-force CV, was determined to decrease exponentially from 30% to 10% as force increased (Moritz et al. 2005).

Excitation E_{in} was modeled as a ramp-and-hold function with a 1 s ramp increase interval and a 5 s constant level. A constant excitation level was set with a mean force of 10% MVC. When all MUs

4

were recruited and were discharging at their maximal firing rates, the maximum force was to be 31,567

au, and MU 1-110 were recruited at 10% MVC (3,150 au). The averaged discharge rate of all active MUs

was 12.9 pps, where the discharge rate of MU 1 was 11.2 pps and that of MU 110 was 13.9 pps.

2.2. Motor unit synchronization

A model of MU synchronization for the 10-Hz PT was implemented based on previous

reports (Taylor et al. 2002; Yao et al. 2000). In these studies, one MU was selected as a reference MU,

and the action potentials discharged by other selected MUs (either randomly chosen (Yao et al. 2000) or

those with similar recruitment thresholds (Taylor et al. 2002)) were synchronized to randomly selected

discharges of the reference MU. In this study, however, in order to synchronize periodically and generate

a 10-Hz oscillation, one reference signal for synchronization (not MU, but an impulse train) was

generated and action potentials discharged by selected MUs were synchronized to the reference signal,

where ISIs of the reference impulse were not regular and varied with a Gaussian distribution with a 100

ms mean (10 Hz) and 10 ms of SD. Because the last-recruited large MU is important for the generation of

tremor (Christakos et al. 2006; Erimaki and Christakos 1999), the MUs synchronized to the reference

signal were selected in turn from the largest active MU (ex. MU 110, 109, 108 and so on).

It was reported that a large 10-Hz PT showing a large, narrow peak in the force spectrum was

associated with widespread MU correlations, whereas a weak tremor showing a small, broad peak in the

spectrum exhibited uncorrelated or weakly correlated MU firing (Christakos et al. 2006; Erimaki and

Christakos 1999). From these features, we considered two types of MU synchronization parameters to

contribute to the tremor intensity: (1) number of MUs contributing to the synchronizing activity and (2)

synchrony between MUs contributing to the synchronizing activity.

To manipulate the number of MUs contributing to the synchronizing activity, two model parameters were adjusted: (1) the maximum number of MUs that is able to synchronize to the reference signal and (2) a permissible time interval between action potentials and the reference impulse (Taylor et al. 2002; Yao et al. 2000). To be selected as the action potential contributing to the tremor generation, an MU must have been between the largest active MU and the i-th MU (i = 110 − (maximum number − 1)) and must discharge an action potential within a permissible interval of the reference discharge. For the maximum number, 10%, 25% and 40% of active MUs were considered. For the permissible time interval, 50 ms (almost no limits (Yao et al. 2000)), 30 ms and 15 ms (Taylor et al. 2002) were investigated.

To change the synchrony between MUs, the temporal alignment of selected discharges with the reference impulse was not exactly coincident. The synchrony with the reference impulse varied based on a Gaussian distribution with a 0 ms mean and various SDs (Taylor et al. 2002; Yao et al. 2000). The SD was varied from a physiologically appropriate level (2 ms (Yao et al. 2000)) to a less correlated level: SDs examined were 2 ms, 10 ms and 20 ms.

Finally, as shown in Fig. 1, the following three simulation parameters were varied for the MU synchronization and compared with a no-synchrony condition: (1) the maximum number of MUs that is able to synchronize to the reference signal − 10%, 25% and 40% of active MUs; (2) the permissible time intervals for synchronization − 15 ms, 30 ms and 50 ms; and (3) the synchrony between MUs − 2 ms, 10 ms and 20 ms of SD.

[Figure 1]

6

2.3. Common rhythmic modulation

In order to examine the influence of the oscillatory excitatory input from the CNS, the simulation was also executed without MU synchronization. The oscillatory excitatory input was achieved by adding an oscillating component to the excitation E_{in}, where the excitation was modulated with a sinusoidal oscillation of 10 Hz under a no-synchrony condition. Three oscillatory levels were examined, with amplitudes of 10%, 20% and 30% of the constant excitation level, and the largest MUs included in the oscillatory excitations for each oscillatory level, respectively, were MU 102−117, MU 94−123 and MU 84−129.

2.4. Simulation procedure

The simulation was implemented in Matlab version 7 (Mathworks, Natwick, MA), and the time resolution of the simulation was 1 ms. In the first step, the no-synchrony condition was simulated and the train of action potentials of each MU was saved. In the next step, the conditions of MU synchronization were executed using the saved action potential trains; that is, the discharge adjustment processes for synchronization, explained in the section on motor unit synchronization in the Methods chapter, were performed using the action potentials of the no-synchrony condition. The oscillatory input condition was simulated based on the no-synchrony condition. Each test condition was run 10 times.

2.5. Data analysis

The aim of this study was to evaluate the causal relation between the 10-Hz and lower frequency fluctuations, and these fluctuations were analyzed separately. To compare fluctuation amplitudes, both fluctuations were defined with SD. The fluctuation around 10 Hz (10-Hz fluctuation) was defined with the SD, where the original data were band-pass filtered with a range between 5 Hz and 18 Hz. The lower frequency fluctuation (LF fluctuation) was the SD in the lower frequency range, where the original data were low-pass filtered with a cut-off frequency of 5 Hz. As for the analysis period of one simulation, in order to exclude the data of the ramp section, the data from 4,096 samples over 1.8 s were used.

Because a peak corresponding to the mean discharge rates appeared clearly in the power spectrum (Taylor et al. 2003), peak amplitudes around 10 Hz and the component corresponding to the mean discharge rate (around 13 Hz) were further examined. These two frequencies were too close to separate with the filter technique, so the two components were examined in the power spectrum. The power spectrum was calculated using a fast Fourier transform (FFT) algorithm, where the data were divided into two blocks of 2,048 samples each (frequency resolution was approximately 0.5 Hz). The peak amplitudes of the 10-Hz and 13-Hz components were obtained from the averaged power spectrum to improve the S/N ratio (two blocks and 10 simulations, 20 blocks in total).

2.6. Statistical analysis

Influences of the MU synchronization parameters on the fluctuations were compared with two-way analysis of variance (ANOVA). Influences of the oscillatory excitation were tested with one-way ANOVA. The Bonferroni test was used for a post-hoc multiple comparison test. The Pearson correlation

coefficient was calculated to examine the relation between the 10-Hz and LF fluctuations. Statistical

analysis was performed with SPSS v.16 (SPSS Inc.).

3. Results

The number of MUs contributing to MU synchronization, stratified by maximum number of

MUs and permissible time intervals, are shown in Table 1. As the maximum number and the permissible

time interval became larger, the number of MUs increased. If the permissible time interval was not

considered, that is, if all MUs (maximum number) were synchronized, the numbers of MUs included in

the synchronization were 11, 27 and 44, respectively, at each maximum number range. Therefore, almost

all MUs were synchronized to the reference signal when the permissible time interval was 50 ms.

[Table 1]

Examples of simulated data are shown in Fig. 2. Four peaks were observed: less than 5 Hz, at

10 Hz, around 13 Hz, and at 20 Hz. In the no-synchrony condition shown in Fig. 2(A), the LF fluctuation

under 5 Hz appeared, along with a peak around 13 Hz. Under 10-Hz synchronization, a small peak

appeared at 10 Hz (Fig. 2(B)). Under the highest level of synchronization, a large peak appeared at 10 Hz

and the LF fluctuation became larger (Fig. 2(C)). Though a peak appeared around 20 Hz, it was

considered to be a harmonic of 10 Hz, because a sharper 20-Hz peak appeared in the 10-Hz oscillatory

excitatory input condition (Fig. 2(D))

[Figure 2]

Amplitudes of the 13-Hz component changed less than those of the 10-Hz component. Figure 3 shows the changes in amplitude of the 10-Hz and 13-Hz components obtained from the FFT power spectrum. Though the amplitudes of the 10-Hz component changed dramatically depending on the simulation condition, the amplitudes of the 13-Hz component were always around 10 au.

[Figure 3]

Because the changes in amplitude of the 13-Hz component were smaller than those of the 10-Hz component, the influence of the 13-Hz component on fluctuation was considered to be neglegible. Figure 4 shows the relation between the FFT peak amplitudes of the 10-Hz component and the SD of the 10-Hz fluctuation. The high correlation observed between these two values. Therefore, the tremor intensity could be represented by the SD of the 10-Hz fluctuation (band-pass filtered data between 5 Hz and 18 Hz), though it contains the 13-Hz component.

[Figure 4]

3.1. Motor unit synchronization

The 10-Hz and LF fluctuations calculated under the 2-ms MU synchrony condition are shown

in Fig. 5. The amplitudes of both fluctuations increased in parallel with the number of MUs contributing to MU synchronization. Influences of the maximum number (x-axis) and the permissible time interval (plots) on the fluctuations were compared with two-way ANOVA. There was an interaction between two parameters ($F_{(6, 120)} = 516.96$, $p < 0.001$ for the 10-Hz fluctuation; $F_{(6, 120)} = 2.99$, $p < 0.01$ for the LF fluctuation). A post-hoc test showed that as the maximum number (x-axis) and the permissible time interval (plots) became larger, the fluctuations increased. However, though the increase of the 10-Hz fluctuation was evident (Fig. 5(A)), the increase of the LF fluctuation was small (Fig. 5(B)). The same tendency was observed with the 10-ms and 20-ms MU synchronies, though the effects on the increase in fluctuation amplitude became slightly weaker.

[Figure 5]

In contrast to the maximum number of MUs contributing to MU synchronization, different MU synchrony conditions had varying influences on fluctuations. Variations in maximum number of MUs under a 50-ms permissible time interval condition are shown in Fig. 6. There was an interaction between the maximum number of MUs and MU synchrony durations for the 10-Hz fluctuation ($F_{(6, 120)}$ = 419.63, $p < 0.001$), but no interaction was observed for the LF fluctuation. The influence of MU synchrony (plots) on the 10-Hz fluctuation were similar to those of the maximum number of MUs and the permissible time interval, where the 10-Hz fluctuations increased with greater MU synchrony (Fig. 6(A)). However, the LF fluctuations did not change with MU synchrony. As indicated in Fig. 6(B), significant differences were observed only between maximum number pairs (ex. 10% vs. 25% and 10% vs. 40% under the 10-ms MU synchrony condition), and no significant differences were observed between MU

synchrony pairs. These results were the same in the 15-ms and 30-ms permissible time interval conditions.

[Figure 6]

3.2. Common rhythmic modulation

Fluctuations in the conditions of the oscillatory excitatory input are shown in Fig. 7. One-way ANOVA showed that there were significant differences in the fluctuations ($F(3, 40) = 3495.66$, $p < 0.001$ for the 10-Hz fluctuation; $F(3, 40) = 15.55$, $p < 0.001$ for the LF fluctuation). Though the 10-Hz fluctuations increased as the amplitude of oscillatory input increased, the LF fluctuations were less affected.

[Figure 7]

Finnaly, the relation between the amplitudes of the 10-Hz and LF fluctuations is summarized in Fig. 8. Because the effect of MU synchrony conditions on fluctuations differed from that of the maximum number of MUs and the permissible time interval, MU synchrony levels were plotted using different symbols, and two other parameters, the maximum number of MUs and the permissible time interval, were plotted without distinction. In general, it was shown that LF fluctuations increased along with 10-Hz fluctuations. However, the degree of increase strongly depended on the conditions involved.

[Figure 8]

4. Discussion

The purpose of this study was to examine the relation between the amplitudes of the 10-Hz and lower frequency components of force fluctuations. Because the generation mechanisms of these fluctuations are different, it was difficult to use a single MU firing property to explain the relation between these fluctuations.

Using a computer simulation, Yao et al. (2000) demonstrated that MU synchronization increased fluctuations. If the time interval in which MUs were synchronized was indeterminate rather than constant, fluctuations occurred and fluctuation amplitudes increased with the number of MUs in synchrony, though the average force was not influenced. In their report, however, synchronization timing was not periodic but random. Therefore, no periodic components were included in the fluctuations and the increase in fluctuations was not considered to relate to a specific frequency component. In this study, therefore, the synchronization was limited to periodic timing (10 Hz) and the LF fluctuation was analyzed separately from the 10-Hz component.

4.1. Comparison between simulated and experimental results

We previously reported that there was a correlation between the 10-Hz and LF fluctuations in

finger force PT experiments (Endo and Kawahara 2010). In this prior study, the force data were first-order differentiated to decrease the attenuation in the frequency domain and enhance FFT peaks of the 10-Hz PT. The force data obtained previously were reanalyzed using the methods employed in simulation, that is, measured data (not differentiated) were band-pass filtered and SD was calculated for the LF fluctuation. As shown in Fig. 9, a slope of the simulation results of the 2-ms MU synchrony condition (see also Fig. 8), which is a physiologically appropriate level (Yao et al. 2000), were closest to the experimental results. Because the target force levels differed between the simulated and experimental results, ranges of the 10-Hz fluctuation were different. However, regression lines corresponded closely.

[Figure 9]

4.2. Influence of MU synchronization

It was reported that the large 10-Hz PT was accompanied by (1) greater MU synchrony and (2) a larger number of synchronizing MUs (Christakos et al. 2006; Erimaki and Christakos 1999). Therefore, two parameters were considered to change the amplitude of the 10-Hz fluctuation: (1) the synchrony with the reference signal and (2) the number of MUs contributing to the 10-Hz PT. In addition, the number of MUs contributing to the 10-Hz PT changed with the maximum number of MUs synchronized with the reference signal and the permissible time interval between action potentials and the reference impulse (Taylor et al. 2002; Yao et al. 2000).

As expected, these three parameters strongly influenced the 10-Hz fluctuation. When the maximum number of MUs considered for synchronization and the permissible time interval for

14

synchronization became larger, the amplitude of the 10-Hz fluctuation became larger. In addition, the higher the MU synchrony, the larger the amplitude of the 10-Hz fluctuation. Because these parameters cause a higher number of action potentials to closely approach the reference impulse, the amplitude of the 10-Hz fluctuation increases.

The LF fluctuation was influenced by the number of MUs contributing to the 10-Hz PT amplitude, though the changes in the LF fluctuation amplitude were not large. On the contrary, the synchrony between MUs did not influence the LF fluctuation at all (Fig. 6(B)). As shown in Fig. 8, even when the SD of the MU synchrony changed from 2 ms to 20 ms, the range of the LF fluctuation did not change (the range of changes was approximately between 50 au and 80 au). Therefore, it was the number of MUs contributing to the amplitude of the 10-Hz PT and not the MU synchrony that was considered to be a plausible explanation for the correlation between the 10-Hz and LF fluctuations under the current simulation parameters.

Yao et al. (2000) reported that the fluctuations (SD and the total power in the FFT) increased when larger number of MUs were included in the synchronization (specifically, their study compared moderate synchrony with high synchrony). Taylor et al. (2003) also reported that there were differences in SD between the synchrony and no-synchrony conditions over 50% MVC. However, the synchronization in these reports occurred in an indeterminate time interval and no discrimination was performed in the frequency range. It was then unclear how the synchronization influenced the fluctuations in the frequency domain. The present results indicated that the MU synchronization in a certain frequency range increases the fluctuations not only at the synchronizing frequency but also at the lower frequencies.

4.3. Influence of oscillatory excitatory input

In addition to MU synchronization, the oscillatory excitatory input from the CNS is considered to a source of the 10-Hz PT (McAuley et al. 1997; Raethjen et al. 2002; Wessberg and Vallbo 1996). Taylor et al. (2003) demonstrated that though 20-Hz oscillatory input did not change the fluctuation compared with a no-oscillatory input condition, 1-Hz and 12-Hz oscillatory input increased the fluctuation. However, as mentioned earlier, no discrimination in the frequency range was done in their study, and it was unclear whether the increase in fluctuation was due to the oscillatory input itself or not. The present results indicated that though the oscillatory input strongly influenced the amplitude of the 10-Hz fluctuation, there was less effect on the LF fluctuation (Figs. 7 & 8).

Considering the results of the MU synchronization and oscillatory input, it was difficult to explain an increase in LF fluctuation simply by virtue of an increase in the 10-Hz component. However, because the number of MUs contributing to the 10-Hz PT was the only plausible parameter in the current simulation, the following reason was considered. When MUs are synchronized, action potentials are gathered from randomly distributed time points into a small time interval. Then, when a greater number of MUs are synchronized, the distribution of the twitch force becomes distorted and the fused twitch forces realized by random distribution become unfused. Consequently, the LF fluctuation is believed to increase.

4.4. Influence of visual feedback

It was reported that when the force-holding task was performed without visual feedback, fluctuations tended to decrease (Baweja et al. 2009; Taylor et al. 2003; Tracy 2007). In the frequency

domain, the frequency components of fluctuation lower than 3 Hz showed a significant difference between conditions with and without visual feedback (Baweja et al. 2009). However, the differences were observed under moderate-force conditions, and no difference was observed when the task was performed under low-force conditions (Baweja et al. 2009). It was reported that fluctuations and control strategy were differed between moderate and weak force levels (Moritz et al. 2005; Sosnoff et al. 2006; Taylor et al. 2003). Though visual feedback was not considered in the present simulation, the target force was the low-force condition. Therefore, the influence of visual feedback was considered to be small, if present at all.

5. Conclusions

Up to this point, the 10-Hz and LF components of the PT have been discussed separately and different mechanisms were proposed for each, and it has been difficult to account for both fluctuations simultaneously using the same MU firing property. This led to the challenge of explaining the relation between the 10-Hz and LF fluctuations.

In this study, attempted to do this by including the generation mechanisms of the 10-Hz PT in the MU force fluctuation model. Our computer simulation showed that the only plausible factor to explain the correlation between the 10-Hz and LF fluctuations was the number of MUs considered to synchronize with the reference signal (10-Hz PT timing). The MU synchrony and the oscillatory excitatory input from the CNS failed to explain the relation between the 10-Hz and LF fluctuations. The finding that MU synchronization influences the fluctuation in the LF range provides new insight into the generation of

force fluctuations.

References

Allum JH, Dietz V, Freund HJ (1978) Neuronal mechanisms underlying physiological tremor. J Neurophysiol 41: 557-571

Baweja HS, Patel BK, Martinkewiz JD, Vu J, Christou EA (2009) Removal of visual feedback alters muscle activity and reduces force variability during constant isometric contractions. Exp Brain Res 197: 35-47

Christakos CN, Papadimitriou NA, Erimaki S (2006) Parallel neuronal mechanisms underlying physiological force tremor in steady muscle contractions of humans. J Neurophysiol 95: 53-66

Elble RJ (1996) Central mechanisms of tremor. J Clin Neurophysiol 13: 133-144

Elble RJ, Randall JE (1976) Motor-unit activity responsible for 8- to 12-Hz component of human physiological finger tremor. J Neurophysiol 39: 370-383

Endo H, Kawahara K (2010) Relationship between hand stability and the 10-Hz physiological tremor during various manual tasks. Ergonomics 53: 491-501

Erimaki S, Christakos CN (1999) Occurrence of widespread motor-unit firing correlations in muscle contractions: their role in the generation of tremor and time-varying voluntary force. J Neurophysiol 82: 2839-2846

Fuglevand AJ, Winter DA, Patla AE (1993) Models of recruitment and rate coding organization in motor-unit pools. J Neurophysiol 70: 2470-2488

Halliday DM, Conway BA, Farmer SF, Rosenberg JR (1999) Load-independent contributions from motor-unit synchronization to human physiological tremor. J Neurophysiol 82: 664-675

Laidlaw DH, Bilodeau M, Enoka RM (2000) Steadiness is reduced and motor unit discharge is more variable in old adults. Muscle Nerve 23: 600-612

McAuley JH, Marsden CD (2000) Physiological and pathological tremors and rhythmic central motor control. Brain 123: 1545-1567

McAuley JH, Rothwell JC, Marsden CD (1997) Frequency peaks of tremor, muscle vibration and electromyographic activity at 10 Hz, 20 Hz and 40 Hz during human finger muscle contraction may reflect rhythmicities of central neural firing. Exp Brain Res 114: 525-541

Miyake S, Loslever P, Hancock PA (2001) Individual differences in Tracking. Ergonomics 44: 1056-1068

Moritz CT, Barry BK, Pascoe MA, Enoka RM (2005) Discharge rate variability influences the variation in force fluctuations across the working range of a hand muscle. J Neurophysiol 93: 2449-2459

Raethjen J, Lindemann M, Dumpelmann M, Wenzelburger R, Stolze H, Pfister G, Elger CE, Timmer J,

Deuschl G (2002) Corticomuscular coherence in the 6-15 Hz band: is the cortex involved in the generation of physiologic tremor? Exp Brain Res 142: 32-40

Semmler JG, Nordstrom MA (1995) Influence of handedness on motor unit discharge properties and force tremor. Exp Brain Res 104: 115-125

Semmler JG, Nordstrom MA (1998) Motor unit discharge and force tremor in skill- and strength-trained individuals. Exp Brain Res 119: 27-38

Sosnoff JJ, Valantine AD, Newell KM (2006) Independence between the amount and structure of variability at low force levels. Neurosci Lett 392: 165-169

Sowman PF, Türker KS (2005) Methods of time and frequency domain examination of physiological tremor in the human jaw. Hum Mov Sci 24: 657-666

Takanokura M, Sakamoto K (2001) Physiological tremor of the upper limb segments. Eur J App Physiol 85: 214-225

Taylor AM, Christou EA, Enoka RM (2003) Multiple features of motor-unit activity influence force fluctuations during isometric contractions. J Neurophysiol 90: 1350-1361

Taylor AM, Steege JW, Enoka RM (2002) Motor-unit synchronization alters spike-triggered average force in simulated contractions. J Neurophysiol 88: 265-276

Tracy BL (2007) Visuomotor contribution to force variability in the plantarflexor and dorsiflexor muscles. Hum Mov Sci 26: 796-807

Tracy BL, Maluf KS, Stephenson JL, Hunter SK, Enoka RM (2005) Variability of motor unit discharge and force fluctuations across a range of muscle forces in older adults. Muscle Nerve 32: 533-540

Vaillancourt DE, Newell KM (2000) Amplitude changes in the 8-12, 20-25, and 40 Hz oscillations in finger tremor. Clin Neurophysiol 111: 1792-1801

Vasilakos K, Glass L, Beuter A (1998) Interaction of tremor and magnification in a motor performance task with visual feedback. J Mot Behav 30: 158-168

Wessberg J, Vallbo ÅB (1996) Pulsatile motor output in human finger movements is not dependent on the stretch reflex. J Physiol 493: 895-908

Yao W, Fuglevand RJ, Enoka RM (2000) Motor-unit synchronization increases EMG amplitude and decreases force steadiness of simulated contractions. J Neurophysiol 83: 441-452

Figure legends

Fig. 1   Schematic diagram showing three simulation parameters for manipulation of MU synchronization. i = 110 − (maximum number − 1).

Fig. 2   Example of simulated waveform and FFT power spectrum. (A) No-synchrony condition; (B) weak synchronization (maximum number = 25%, permissible time interval = 30 ms, MU synchrony = 10 ms); (C) high synchronization (maximum number = 40%, permissible time interval = 50 ms, MU synchrony = 2 ms); (D) oscillatory excitatory input = 30%. In the FFT power spectrum, spectra of filtered data were also shown. Note: scale of the FFT power spectrum in (D) is different from other spectra.

Fig. 3   Relation between the FFT peak amplitudes of the 10-Hz and 13-Hz components. Plots represent all simulation conditions. A regression line and a correlation coefficient are also shown.

Fig. 4   Relation of the 10-Hz PT intensity between the FFT peak and the SD of the 10-Hz fluctuation. Plots represent each simulation condition. A regression line and a correlation coefficient are also shown.

Fig. 5   The 10-Hz and LF fluctuations calculated under a 2-ms MU synchrony condition. (A) 10-Hz fluctuation; (B) LF fluctuation. Pairs with a significant difference are shown. * and ** indicate $p < 0.05$ and $p < 0.01$ respectively. No sign indicates a significant difference of $p < 0.001$.

Fig. 6   The 10-Hz and LF fluctuations calculated under a 50-ms permission interval condition. (A)

10-Hz fluctuation; (B) LF fluctuation. Pairs with a significant difference are shown. * and ** indicate $p <$ 0.05 and $p < 0.01$ respectively. No sign indicates a significant difference of $p < 0.001$.

Fig. 7   The 10-Hz and LF fluctuations calculated under the oscillatory excitatory input condition. Filled square symbols represent the SD of the 10-Hz fluctuation and white diamonds represent the LF fluctuation.

Fig. 8   Relation of SDs between the 10-Hz and LF fluctuations. The SDs were plotted separately depending on the synchrony between MUs: white square symbols represent the 2-ms MU synchrony condition, filled diamond symbols represent the 10-ms MU synchrony, and white circle symbols indicate the 20-ms MU synchrony. The parameters (the maximum number of MUs and the permissible time intervals) were plotted without distinction. The oscillatory excitatory input conditions were indicated with cross symbols. Regression lines and correlation coefficients are also shown.

Fig. 9   Comparison of fluctuations between simulated and experimental data. The experimental data obtained previously (Endo and Kawahara 2010; averages of right and left index fingers and thumbs, target force = 1 N, n = 35) were plotted with the simulation results of the 2-ms MU synchrony condition. In order to directly compare the x-axes of both sets of results, units of force data were converted into %MVC, where the experimental target force of 1 N was assumed to be 5% MVC for the sake of convenience. The straight lines plotted are regression lines. In the regression equations, x is the 10-Hz fluctuation and y is the LF fluctuation.
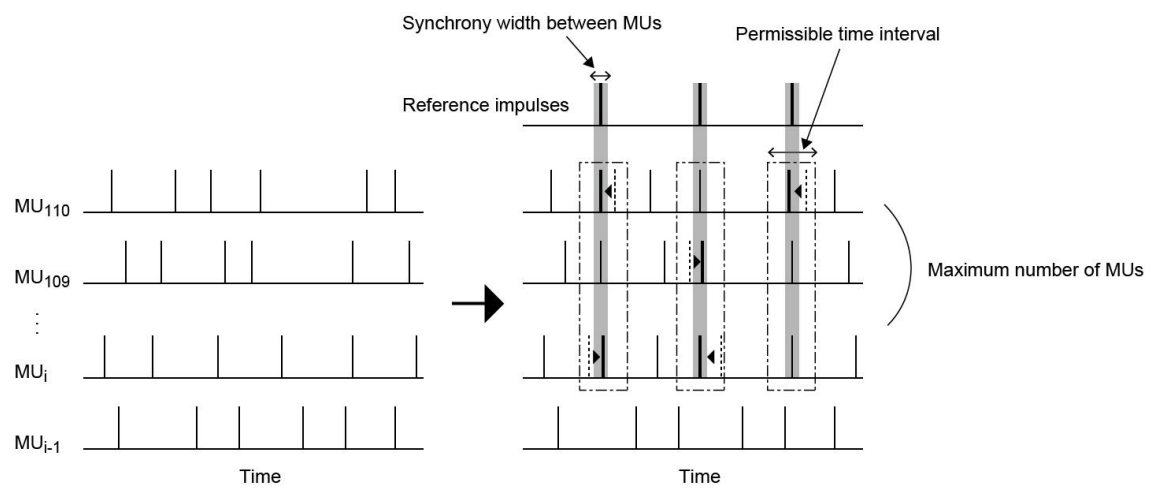
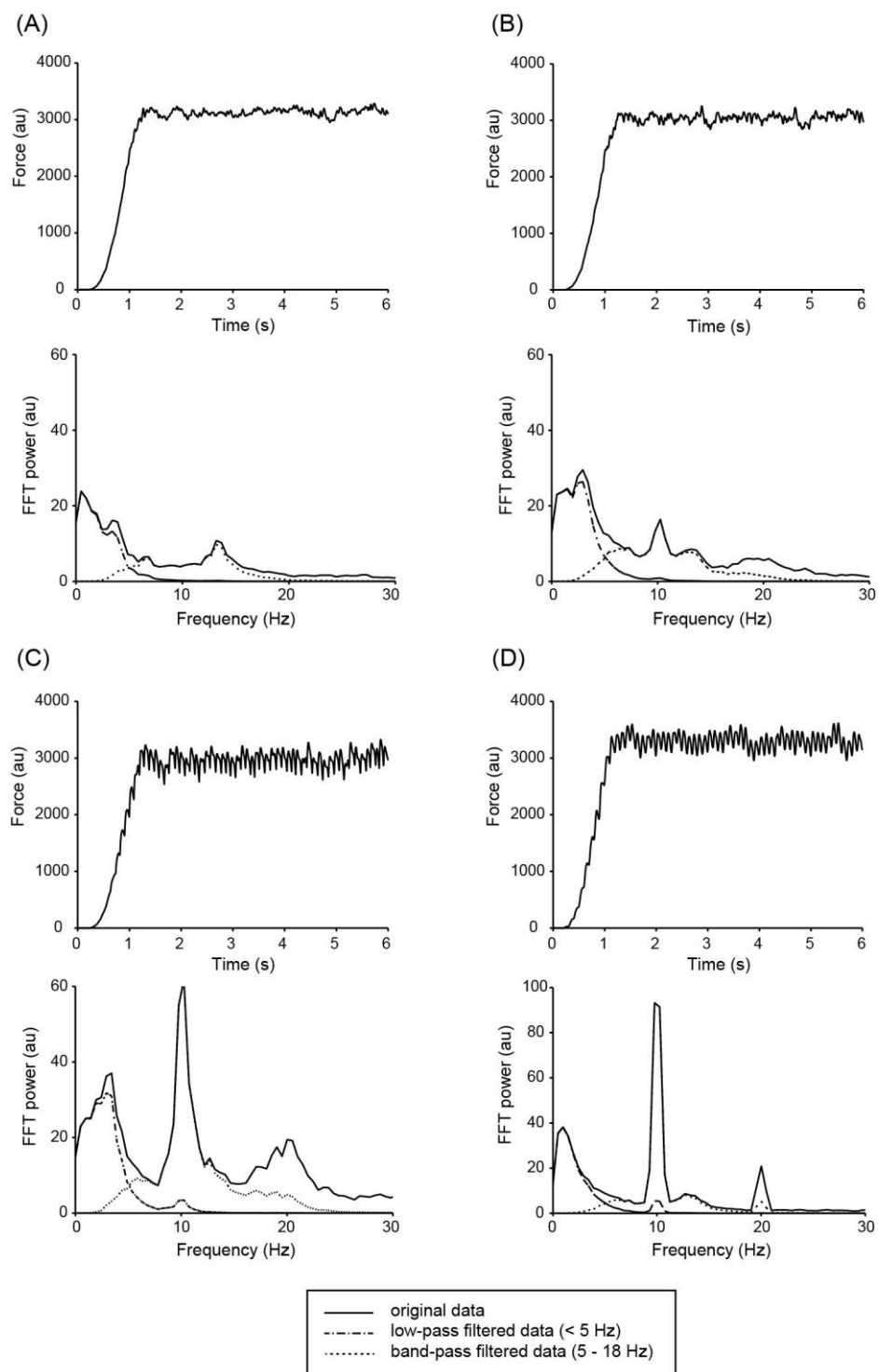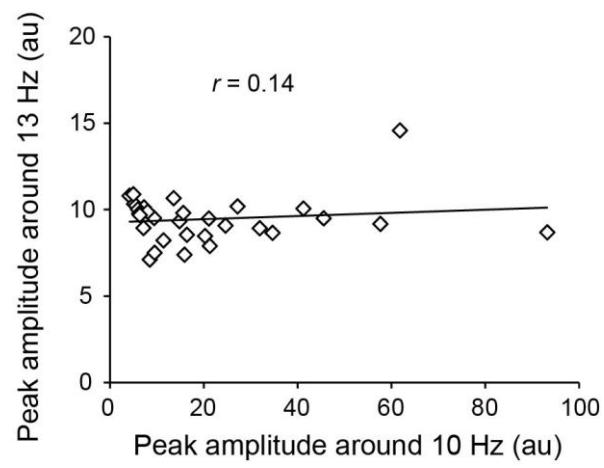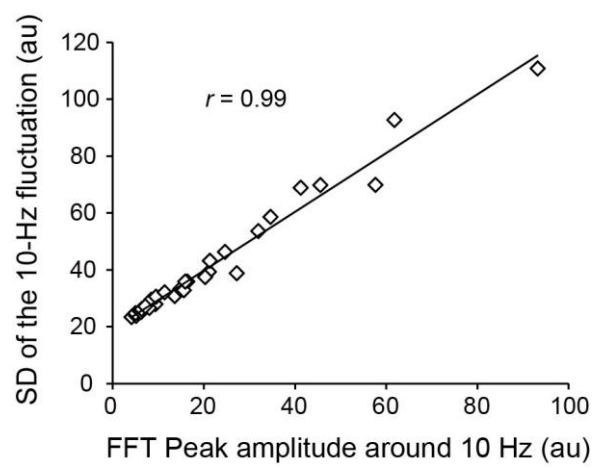Table 1　　Number of MUs contributing to the MU synchronization.
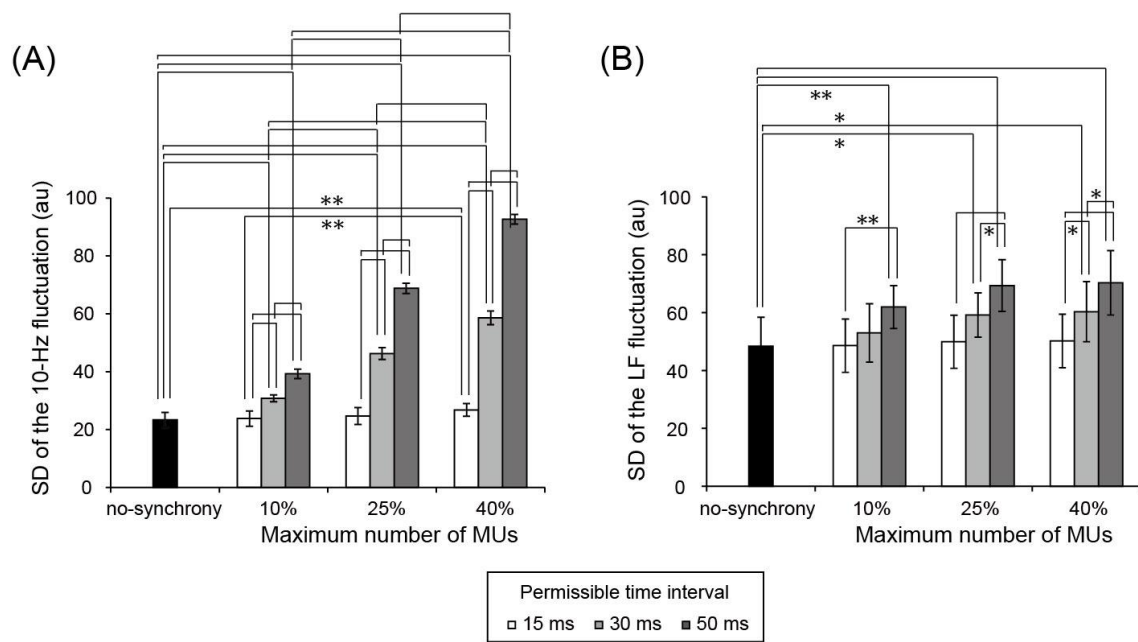
Figure 1

Figure 2

Figure 3
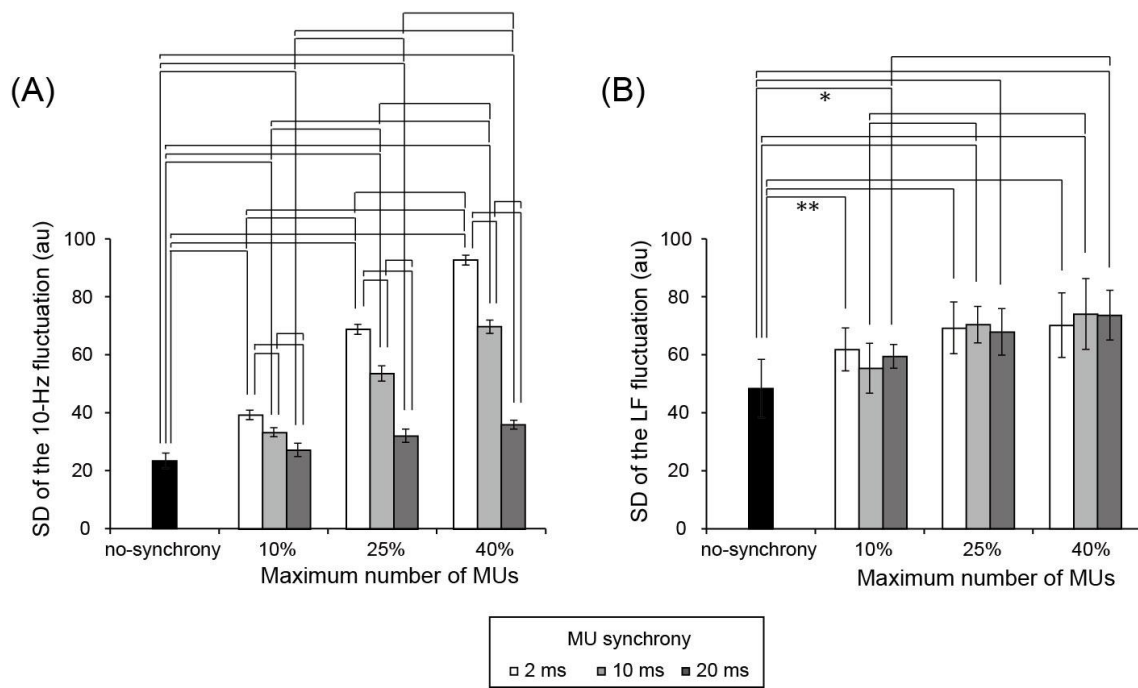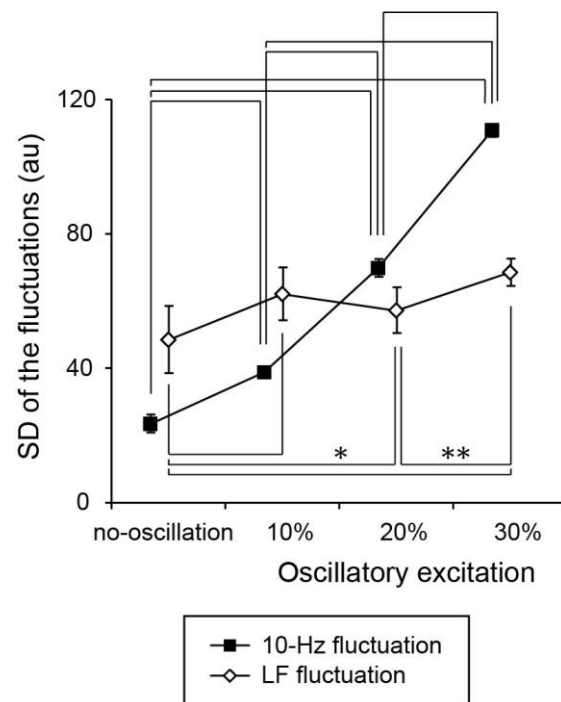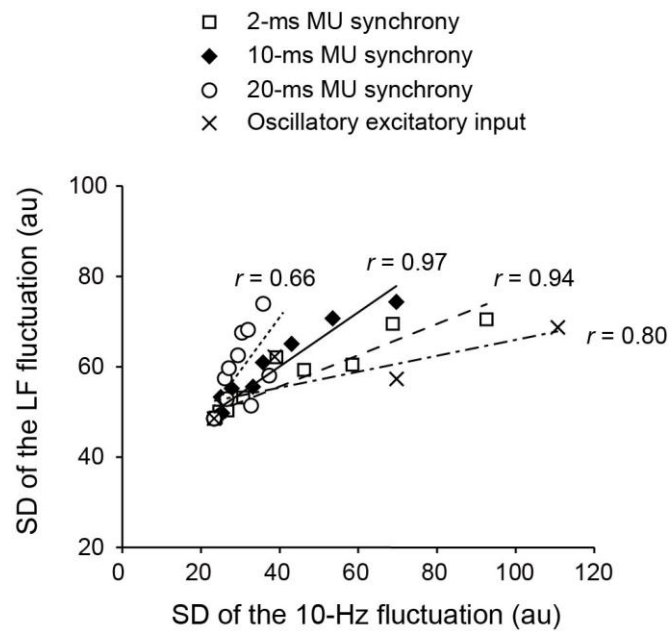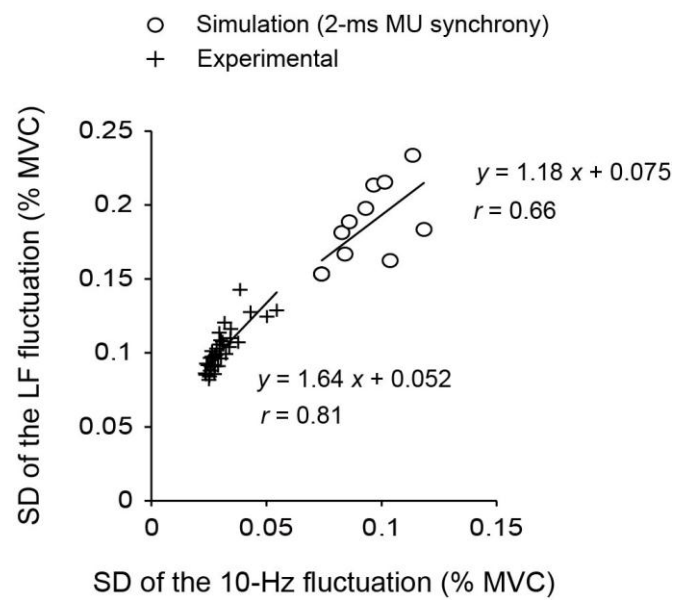

Figure 4

Figure 5

Figure 6

Figure 7

Figure 8

Figure 9

Table 1

Permissible time interval for synchronization	Maximum number of MUs synchronized to the reference signal		
	10%	25%	40%
15 ms	4.6 ± 1.6	11.4 ± 2.6	18.6 ± 3.3
30 ms	8.8 ± 1.3	22.0 ± 2.1	35.9 ± 2.6
50 ms	10.9 ± 0.3	26.9 ± 0.4	43.9 ± 0.4

Note. Mean ± SD.